# Antibody-mediated depletion of CCR10$^{+}$ EphA3+ cells ameliorates fibrosis in IPF.

Miriam S. Hohmann[1], David M. Habiel[1], Milena S. Espindola[1], Guanling Huang[1], Isabelle Jones[1], Rohan Narayanan[1], Ana Lucia Coelho[1], Justin M. Oldham[2], Imre Noth[3], Shwu-Fan Ma[3], Adrianne Kurkciyan[1], Jonathan McQualter[1], Gianni Carraro[1], Barry Stripp[1], Peter Chen[1], Dianhua Jiang[1], Paul W. Noble[1], William Parks[1], John Woronicz[4], Geoffrey Yarranton[4], Lynne A. Murray[5], and Cory M. Hogaboam[1*]

**Affiliations:**

[1]Women's Guild Lung Institute, Division of Pulmonary and Critical Care Medicine, Department of Medicine, Cedars-Sinai Medical Center, Los Angeles, CA, USA, 90048.
[2]Department of Internal Medicine, Division of Pulmonary, Critical Care and Sleep Medicine, University of California at Davis, Sacramento, CA, USA, 95817.
[3]Division of Pulmonary and Critical Care, Department of Medicine, University of Virginia, Charlottesville, VA, USA, 22904.
[4]KaloBios Pharmaceuticals (now Humanigen), Burlingame, CA 94010.
[5]MiroBio Ltd, Winchester House, Heatley Road, Oxford Science Park, Oxford, UK, OX4 4GE.

# Online supplemental materials

37 **Supplemental Methods:**

38 **Immunohistochemistry**

39 Slides containing 4 μm sections were deparaffinized and hydrated by incubating
40 them in two changes of xylene for five min each, followed by 2 changes of 100% ethanol
41 for 3 min each, 70% ethanol for 2 min, 50% ethanol for 2 min, and distilled water for 5
42 min. Antigen retrieval was performed by incubating the slides in 10 mM Citric acid solution
43 (pH 6.0) in an 80 ºC oven overnight. The slides were subsequently washed in PBS and
44 permeabilized in 10% methanol containing 0.4% $H_2O_2$ for 30 min. After permeabilization,
45 slides with murine tissues were washed and stained with a rabbit anti-GFP antibodies
46 and using an aminoethyl carbazole (AEC) substrate kit. IHC analysis on human lung
47 biopsies or explants were performed using a rabbit anti-human CCR10 (Abcam,
48 Ab30718), rabbit anti-CCL28 (Genetex, Inc, GTX108432), rabbit anti-CD68 (Abcam,
49 Ab213363) or rabbit anti-surfactant protein C (Abcam, Ab40879) antibodies. Dual color
50 IHC was performed using a dual color IHC kit (Enzo Lifesciences), rabbit anti-human
51 CCR10 (Abcam, Ab30718) and mouse anti-human EphA3 (Clone, SL2, Humanigen, Inc.)
52 antibodies as recommended by the manufacturer. Immunofluorescence staining was
53 completed by washing the slides following primary antibody incubation and subsequent
54 incubation with fluorescent probe conjugated secondary antibodies for 1 h at room
55 temperature. Slides were then washed and mounted using a DAPI containing mounting
56 medium (Thermo Fisher Scientific). IHC staining for lung fibroblasts was performed as
57 follows: cells were fixed using 4% formaldehyde solution for 10 minutes at room
58 temperature. The cells were then, washed, permeabilized by incubating them in 10%
59 methanol solution for 5 minutes and stained with anti-EphA3 antibodies followed by HRP

60 conjugated secondary antibodies and DAB developing reagent. All images were acquired
61 using an AxioCam MRc camera Zeiss AX10 microscope using a 5x (0.16 aperture) and
62 20x (0.8 aperture) lenses (Carl Zeiss Microscopy GmbH) at room temperature and Zen
63 2012 (Blue edition) v 1.1.2.0 software.
64

65 **Generation of Senescent Fibroblasts**

66 Senescent fibroblasts were generated as previously described(1). Proliferating NL and
67 IPF lung fibroblasts were serially passaged in culture until the cells showed a senescent
68 phenotype (flattened morphology, permanent growth arrest, and altered gene expression
69 [upregulation of *CDKN1A*, *CDKN2A*, *IL6*, and *IL8* genes]) and senescence-associated b-
70 galactosidase activity (b-Galactosidase Staining Kit; BioVision).
71

72 **Fibroblast stimulations**

73 Seven-thousand lung fibroblasts per well were plated into a 96 well plate for soluble
74 collagen 1, IL-6, and in cell αSMA and ß-tubulin ELISA analysis or 2.5 x $10^5$ cells/well
75 were plated onto a 6-well plate for qPCR analysis. Cells treated with CCL28 (200 ng/mL,
76 R&D systems) for 72 hours (Supplemental Figure 4, B-F); or pre-clustered EFNA5-Fc
77 (100 nM for 72 hours; R&D systems; pre-clustered via incubation with anti-his tag
78 antibodies (R&D systems, MAB05-100) at a 1:10 ratio for 20 minutes at room
79 temperature), IgG, and Ephrin A ligand neutralizing EphA3-FC chimeric protein for 72
80 hours (Supplemental Figure 5).

81 **Soluble collagen 1, IL-6, and in cell αSMA and ß-tubulin ELISA analysis**

82 Conditioned supernatants were collected for soluble collagen 1 and IL-6 quantification,
83 and the cells were fixed using 4% paraformaldehyde solution in cell αSMA and ß-tubulin
84 ELISA analysis. Commercial ELISA assays (R&D systems) were performed to quantify
85 IL-6 levels as recommended by the manufacturer. Soluble collagen 1 and in cell αSMA
86 and ß-tubulin ELISA assays were carried out as described previously(2).

87

88 **Western blot**

89 Cells were lysed using cell lysis buffer (Cell Signaling) containing Halt™ Protease and
90 Phosphatase Inhibitor Cocktail (Thermo Fisher Scientific) and briefly sonicated and
91 centrifuged. Protein was quantified from cell lysates using a DC Protein assay (Bio-Rad
92 Laboratories, Inc.). For p-EphA3 quantification, traditional western blot analysis was
93 carried out as previously described(2) using anti-phospho-EphA3 (Cell Signaling,
94 #8862S) and anti-β-tubulin (Abcam, ab6046). CCR10 protein was quantified by capillary
95 western blot using JESS according to the manufacturer's protocol (ProteinSimple, San
96 Jose, CA, USA)(3). Lysed protein samples (1 mg/mL), blocking reagent, wash buffer, anti-
97 CCR10 (Abcam, ab30718) or β-tubulin (Abcam, ab6046), anti-rabbit HRP (R&D systems,
98 HAF008), and chemiluminescent substrate were prepared and loaded into appropriate
99 manufacturer-provided plates. Protein separation and detection was performed
100 automatically on the individual capillaries and analysis was carried out as described by
101 the manufacturer **(**Figure 4C**)**. All reagents used in this system were provided by
102 ProteinSimple.

103

104 **Gene expression array data mining and Ingenuity IPA analysis.**

105 To generate a list of tyrosine kinases not targeted by nintedanib, known nintedanib
106 targets(4) were excluded from analysis and the remaining tyrosine kinases were added
107 to a custom Ingenuity pathway generated from the Ingenuity database. Publicly available
108 gene expression datasets (GSE24206) were mined from NCBI's geo datasets database.
109 Groups were defined as follows –IPF lung explants (n=4) vs normal lungs (n=6). Gene
110 expression values were extracted using NCBI's Geo2R gene expression analysis tool and
111 the expression data were uploaded onto ingenuity IPA. Ingenuity IPA was set to only
112 consider changes in gene expression of 1.5-fold or greater and $p \leq 0.05$. Tyrosine kinase
113 expression values were overlaid onto the custom generated list of tyrosine kinases not
114 targeted by nintedanib to generate Table S2.

115

116 **Fibroblast Proliferation**

117 For fibroblast proliferation, $0.5 \times 10^4$ cells control and $GFP^+Puro^+$ cells (CRISPR-
118 Cas9 mediated CCR10 knockout cells subjected to puromycin selection and FACS
119 sorting for GFP expression) were plated in a 96 well plate (Costar) overnight. Proliferation
120 was assessed every 12 hours over a period of 84 hours at 37 $^oC$, 10% $CO_2$ in the IncuCyte
121 ZOOM live cell imager (Essen Biosciences). The percentage of cell confluence was
122 determined using IncuCyte ZOOM software (Essen Biosciences) as recommended by the
123 manufacturer.

124

125 **Quantification of interstitial Masson's Trichrome blue staining:**

126 Lung tissues were Masson's trichrome stained and tile images of the stained NSG

127 lungs were acquired at 10x magnification using a Zeiss AX10 microscope. Images were
128 then stitched and exported using Zen 2012 (blue edition) v 1.1.2.0 software. The exported
129 images were imported into Image pro premier v9.3.3, gamma set to 0.364 and a low pass
130 2D filter was applied (strength 100, passes 65) to blur the image. Using a manual count-
131 threshold and size exclusion filter, airway and large blood vessel (but not interstitial)
132 Masson's trichrome blue staining was detected (Supplemental Figure 14A). The stained
133 areas were then copied as regions of interest (airway ROI) and superimposed onto the
134 original (non-blurred) version of the same lung. Using a manual count-threshold for
135 interstitial blue staining (Supplemental Figure 14, B-C), interstitial collagen-blue staining
136 was quantified outside the airway ROIs and the total stained areas were then exported.
137 The software was set to quantify total lung tissue outside the airway ROIs (Supplemental
138 Figure 14D). Total area of lung tissue was exported and the ratio of total area of trichrome
139 stained regions by total area of lung tissue was calculated using Microsoft Excel
140 (Microsoft Corporation).
141

142 **Detection of IL-12p70, IFNγ and TNFα in the BAL from non-humanized and**
143 **humanized NSG mice.**

144 Lungs in non-humanized and humanized NSG mice were washed using 1 mL of
145 saline solution, and the resulting BAL was centrifuged to remove cells and the
146 supernatants were stored at -80 $^{o}$C until analysis. Mouse cytokines in the BAL were
147 measured using predesigned Bioplex assays (Bio-Rad Laboratories, Inc.) as
148 recommended by the manufacturer.

149 **Supplemental References:**


150 1. Hohmann MS, Habiel DM, Coelho AL, Verri WA, Jr., and Hogaboam CM. Quercetin
151 Enhances Ligand-induced Apoptosis in Senescent Idiopathic Pulmonary Fibrosis
152 Fibroblasts and Reduces Lung Fibrosis In Vivo. *Am J Respir Cell Mol Biol.* 2019;60(1):28-
153 40.
154 2. Espindola MS, Habiel DM, Narayanan R, Jones I, Coelho AL, Murray LA, et al. Targeting of
155 TAM Receptors Ameliorates Fibrotic Mechanisms in Idiopathic Pulmonary Fibrosis. *Am J*
156 *Respir Crit Care Med.* 2018.
157 3. Harris VM. Protein detection by Simple Western analysis. *Methods Mol Biol.*
158 2015;1312:465-8.
159 4. Hilberg F, Roth GJ, Krssak M, Kautschitsch S, Sommergruber W, Tontsch-Grunt U, et al.
160 BIBF 1120: triple angiokinase inhibitor with sustained receptor blockade and good
161 antitumor efficacy. *Cancer Res.* 2008;68(12):4774-82.
162 5. Guo M, Wang H, Potter SS, Whitsett JA, and Xu Y. SINCERA: A Pipeline for Single-Cell
163 RNA-Seq Profiling Analysis. *PLoS Comput Biol.* 2015;11(11):e1004575.
164 6. Du Y, Guo M, Whitsett JA, and Xu Y. 'LungGENS': a web-based tool for mapping single-
165 cell gene expression in the developing lung. *Thorax.* 2015;70(11):1092-4.
166 7. Du Y, Kitzmiller JA, Sridharan A, Perl AK, Bridges JP, Misra RS, et al. Lung Gene
167 Expression Analysis (LGEA): an integrative web portal for comprehensive gene
168 expression data analysis in lung development. *Thorax.* 2017;72(5):481-4.

169

170

171 **Supplemental Figures and Legends:**

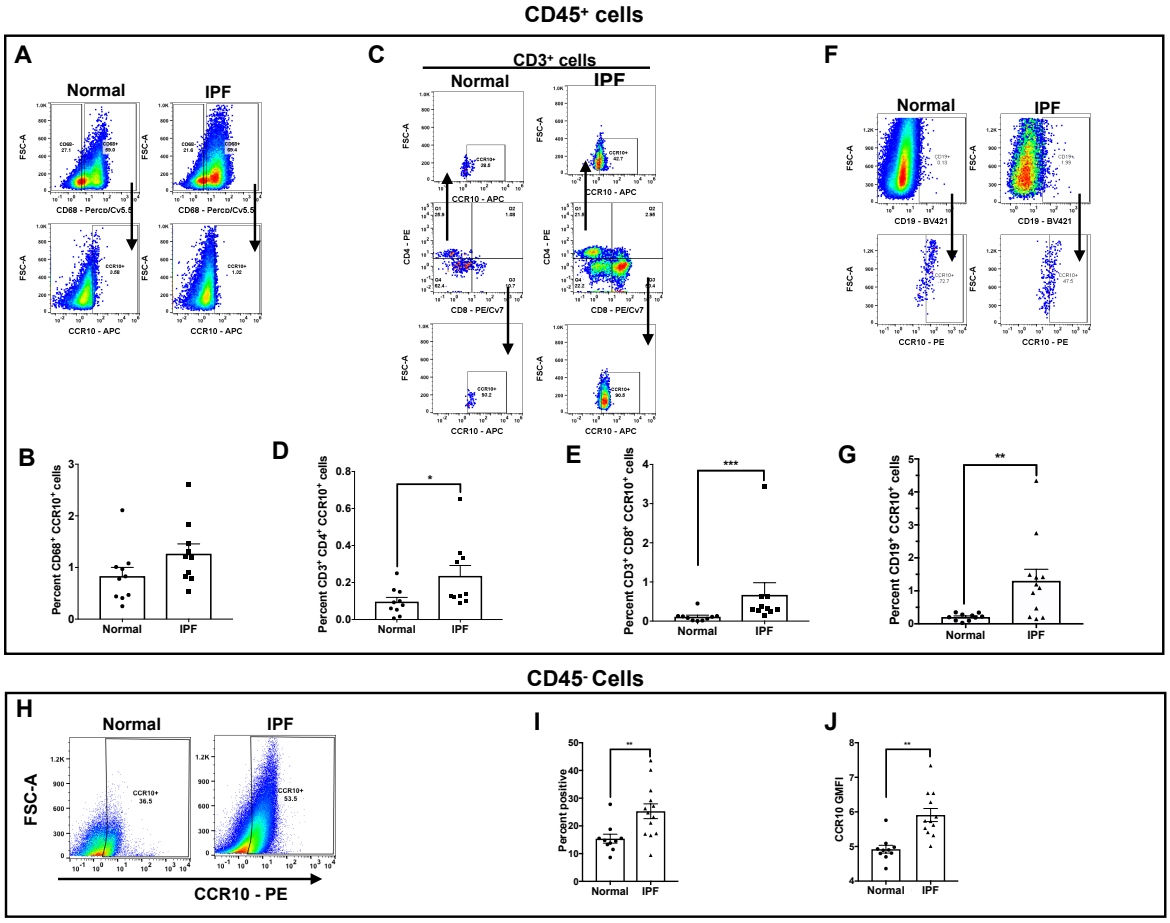


172

173 ***Supplemental Figure 1: Flow cytometric characterization of CD45+ CCR10+ cells in***

174 ***normal and IPF lung explants.***

175 Normal and IPF lung explant cells were stained with anti-CD45, -CCR10, -CD68, -CD3, -

176 CD4, -CD8, and/or -CD19 antibodies and subsequently analyzed by flow cytometry.

177 Depicted are representative flow cytometric dot plots for CCR10 expressing CD68+ (**A**),

178 CD4$^+$, CD8$^+$ (**C**), and CD19$^+$ (**F**) immune cells (CD45$^+$ cells) in normal and IPF lung

179 explants. The average percentage of CD45$^+$ cells expressing CD68$^+$ CCR10$^+$ (**B**), CD3$^+$

180 CD4$^+$ CCR10$^+$ (**D**), CD3$^+$ CD8$^+$ CCR10$^+$ (**E**), and CD19$^+$ CCR10$^+$ (**G**). (**H**) Depicted are

181 representative flow cytometric dot plots for CCR10 expressing CD45$^-$ cells, (**I**) average

182 percentage of CCR10$^{+}$ and CCR10 GMFI in normal and IPF explant cells. Data shown

183 are mean ± s.e.m.; n=10-12/group *p ≤ 0.05; **p ≤ 0.01; ***p ≤ 0.001 via two-tailed Mann

184 Whitney non-parametric test.

185

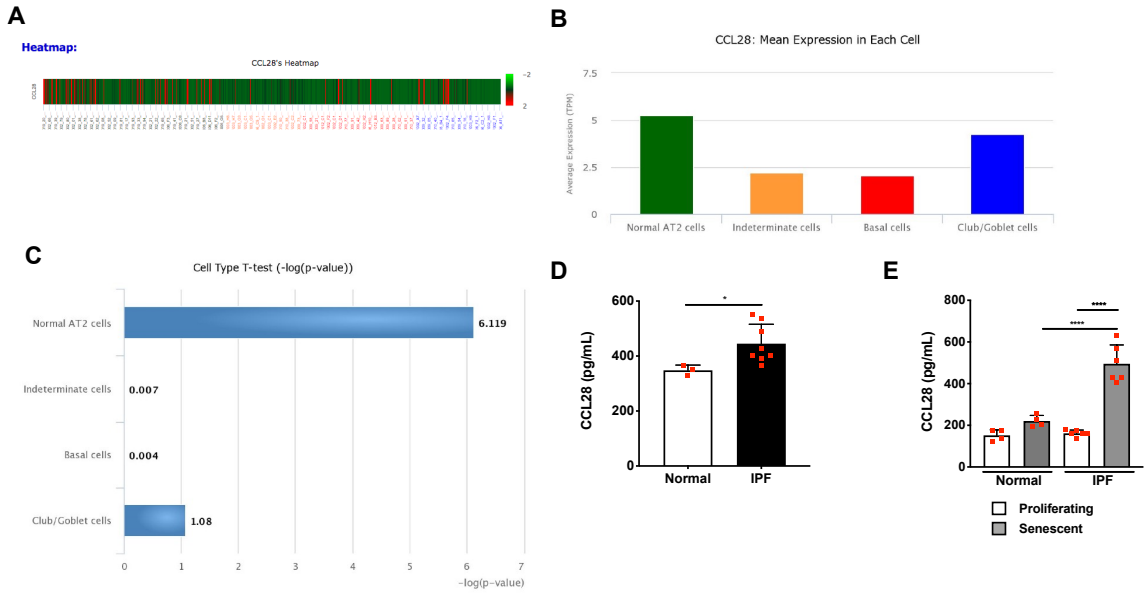


186

187 ***Supplemental Figure 2. CCL28 expression in the lung and tissue derived cultured***

188 ***cells from normal and IPF patients.***

189 (**A-C**) Publicly available single cell RNAseq datasets(5-7) of normal type II alveolar

190 epithelial cells (AT2 cells) and IPF epithelial cells were mined for CCL28 transcript

191 expression. Depicted is a heat map (**A**), average TPM expression (**B**) and the –log(p-

192 value) (**C**) for CCL28 transcript expression in normal and IPF epithelial cells. CCl28 levels

193 in the supernatant of cultured epithelial cell (**D**) from normal (n=3) and IPF (n=8) lung

194 explants. Data shown are mean ± s.e.m.; *p ≤ 0.05 via two-tailed Mann Whitney non-

195 parametric parametric test. CCl28 levels in the supernatant of cultured fibroblasts

196 (proliferating or replication-induced senescecent) (**E**) from normal (n=4) and IPF (n=6)

197 patients. ****p ≤ 0.0001 via one-way ANOVA with Tukey's multiple comparisons test.

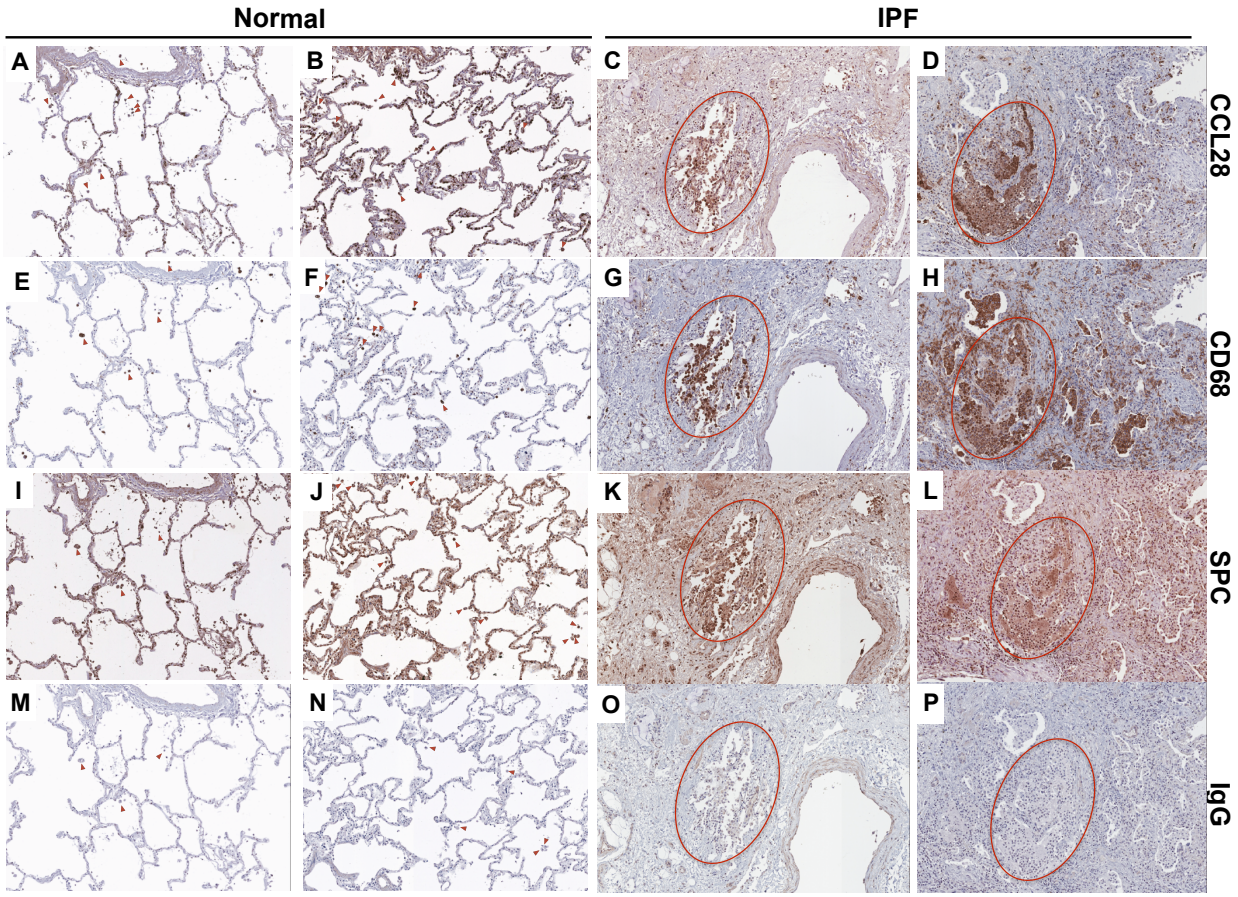


198

199

200 ***Supplemental Figure 3. CCL28 protein expression in normal and IPF lungs.***

201 Representative images of CCL28 (**A-D**), CD68 (**E-H**), SPC (**I-L**), and isotype IgG (**M-P**)

202 staining in normal (**A-B**, **E-F**, **I-J** and **M-N**) and IPF (**C-D**, **G-H**, **K-L** and **O-P**) lung

203 explants. Shown are images taken at 200x magnification. n=7/group.

204

205

206

207

208

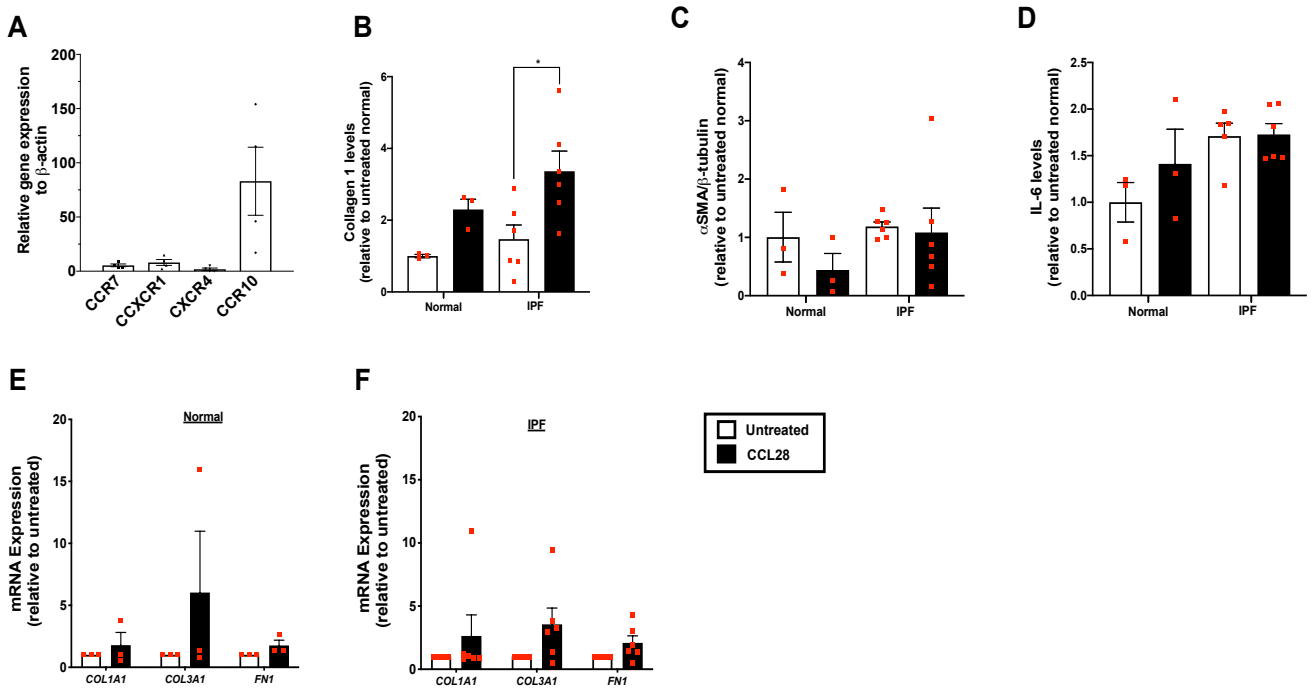


209

210 ***Supplemental Figure 4.*** **IPF lung fibroblasts express CCR10 and CCL28 induces**

211 **minor activation**

212 (**A**) Average expression of *CCR7, CXCR1, CXCR4, and CCR10* transcripts relative to β-

213 actin in IPF lung fibroblasts. Fold change in secreted Collagen 1 (**B**), αSMA/β-tubulin

214 expression (**C**), IL-6 levels (**D**), and fibrosis-related transcripts *COL1A1*, *COL3A1*, and

215 *FN1* in cultured fibroblasts from normal (**E**) or IPF (**F**) patients treated with CCL28 (200

216 ng/mL) for 72 hours. Data shown are mean ± s.e.m.; n= 3-6 fibroblast lines/group. *$p \leq$

217 0.05 via one-way ANOVA with Tukey's multiple comparisons test.

218

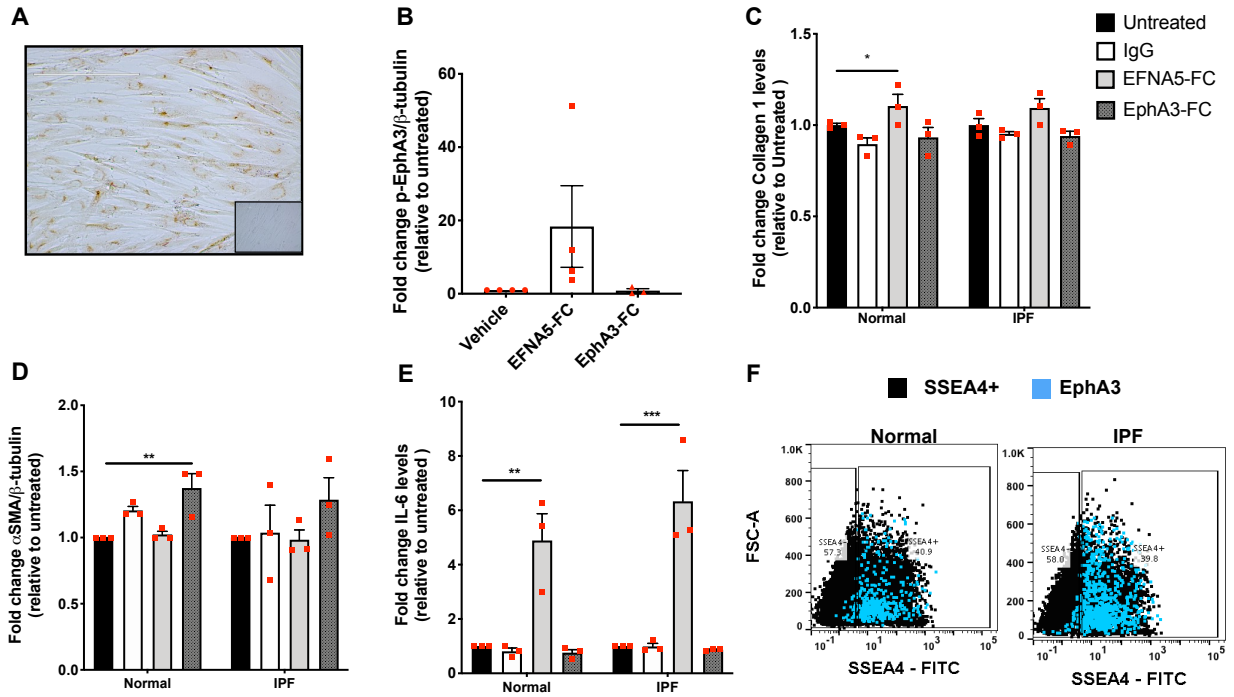


***Supplemental Figure 5. Ephrin A ligand, EFNA5, activates EphA3 and promotes Collagen 1 and IL-6 secretion by lung fibroblasts.***

**(A)** Representative image of EphA3 staining (brown) in IPF lung fibroblasts (inlay = isotype control antibody). **(B)** Fold change of p-EphA3/ß-tubulin protein in fibroblast 30 minutes post stimulation with pre-clustered EFNA5-FC (100 nM) with or without Ephrin A ligand neutralizing EphA3-Fc (200 nM). **(C-F)** Lung fibroblasts were treated with IgG control or pre-clustered EFNA5-FC with or without Ephrin A ligand neutralizing EphA3-Fc for 72 hours and shown is the average fold change in (**C**) soluble collagen 1, (**D**) αSMA, and (**E**) IL-6 protein levels in normal and IPF fibroblasts. (**F**) Flow cytometric dot plots of EphA3 staining (Blue) (APC conjugated anti-EphA3) on gated SSEA4$^{+}$ (FITC conjugated streptavidin & biotinylated anti-SSEA4) cells in cultured normal and IPF lung fibroblasts. Data shown are mean ± s.e.m.; n= 3-4 fibroblast lines/group. *p ≤ 0.05; **p ≤ 0.01; ***p ≤ 0.001 via one-way ANOVA test with Tukey's multiple comparisons test.

233

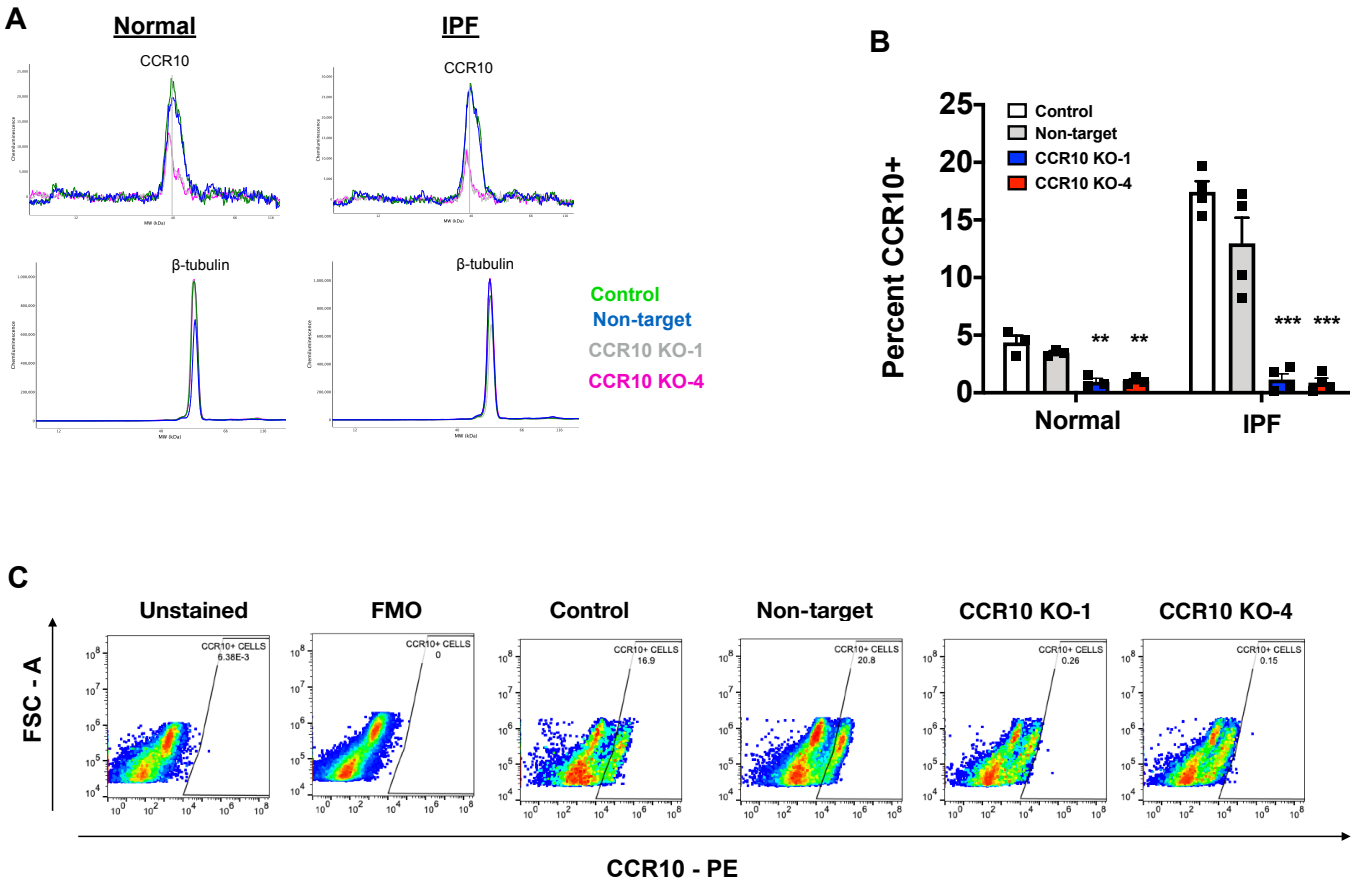


234

235

236 ***Supplemental Figure 6. Validation of CRISPR-Cas9-mediated targeting of CCR10.***

237 **(A)** Representative electropherogram peaks for CCR10 and β-tubulin in control, **(B)**

238 percent CCR10+ cells and **(C)** representative flow cytometric dot plots of CCR10 (PE)

239 expressing cells in control, non-target, and CCR10 KO-1 and 4 fibroblasts, as well as flow

240 cytometric controls. Data shown are mean ± s.e.m.; n= 3-4 fibroblast lines/group. **p ≤

241 0.01; ***p ≤ 0.001 via one-way ANOVA test with Tukey's multiple comparisons test.

242

243

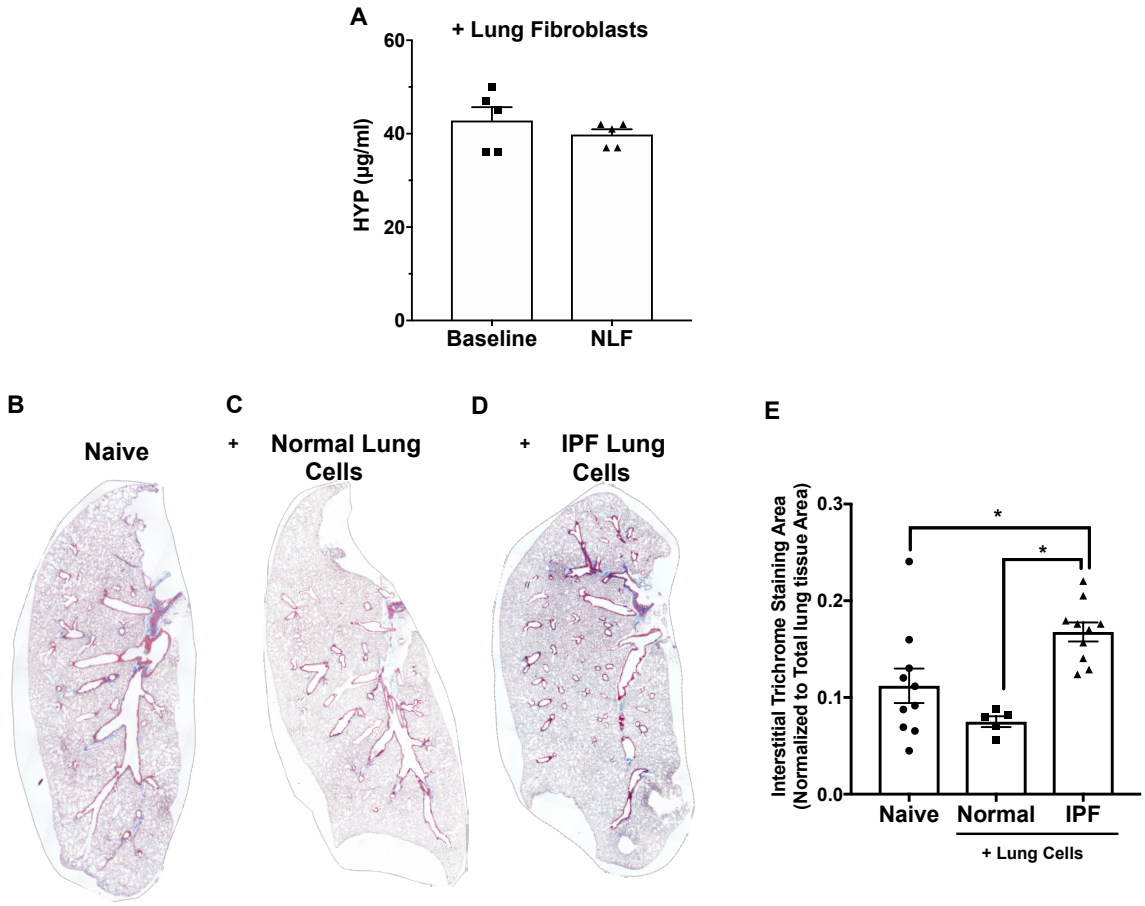


***Supplemental Figure 7. Normal lung fibroblasts and explant cells do not promote interstitial fibrosis in the lungs of humanized NSG mice.***

(**A**) One million cultured normal lung fibroblasts were I.V. administered into SCID-beige mice. Sixty-three days after cellular administration, mice were sacrificed, and their lungs were biochemically assessed for hydroxyproline concentration. Shown is the mean hydroxyproline concentration in the lungs of naïve and normal lung fibroblast challenged mice. (**B-D**) Shown are whole mount Masson's trichrome stained non-humanized (**B**), normal lung explant cell-humanized (**C**) or IPF lung explant cell humanized and control IgG treated (**D**) NSG lungs, 63 days after human cell administration. (**E**) Shown are ratios

255 of the Area sum of interstitial blue trichrome staining normalized to total lung tissue area.
256 n=10 naïve; n=5 normal lung humanized; n=10 IPF lung humanized, IgG control treated
257 NSG lungs. Data shown are mean ± s.e.m.; *p ≤ 0.05 via via one-way ANOVA test with
258 Tukey's multiple comparisons test.
259
260

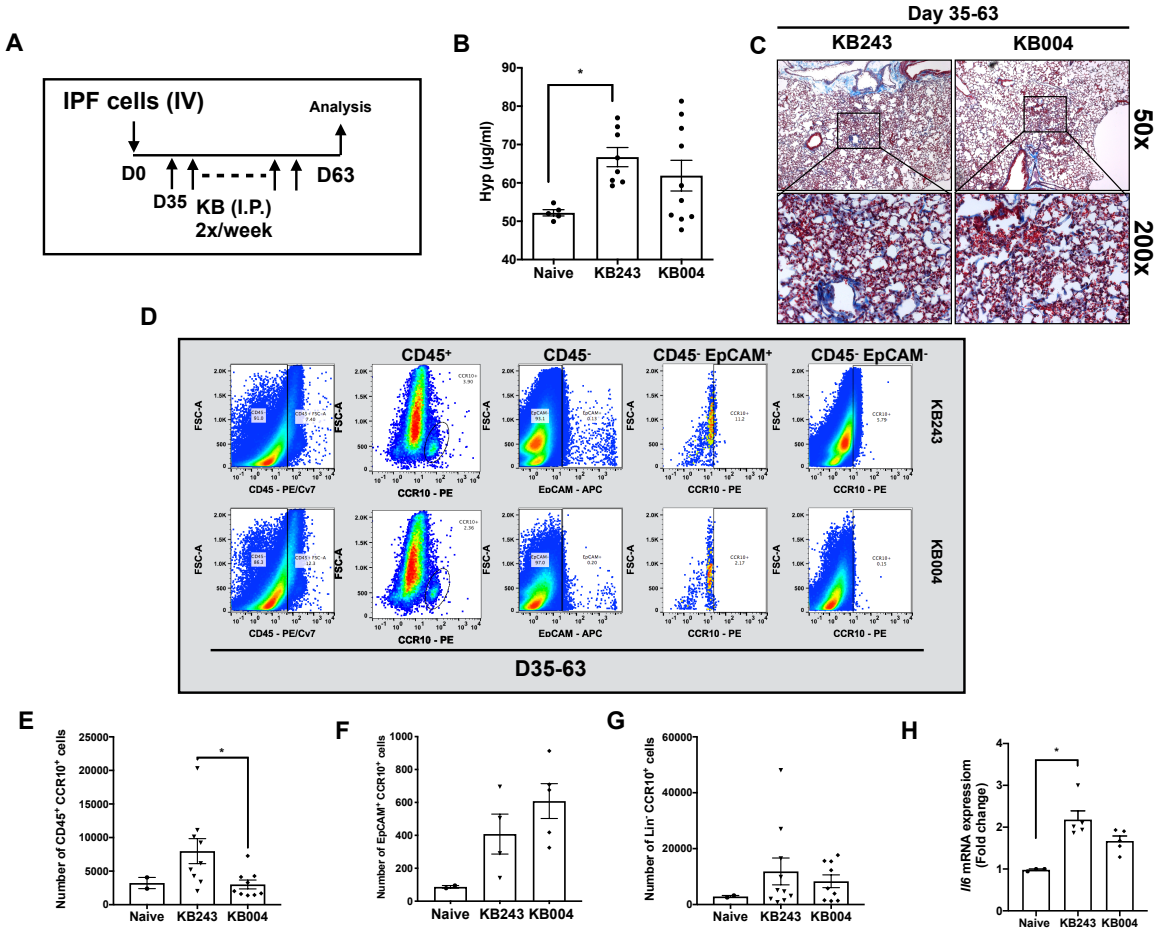


***Supplemental Figure 8. Therapeutic administration of KB004 did not reduce established pulmonary fibrosis in humanized NSG mice.***

**(A)** Experimental scheme. **(B)** Hydroxyproline in lungs from humanized NSG mice treated with either KB243 or KB004 mAbs. Data shown are mean ± s.e.m.; n=5-10/group. *$p \leq 0.05$ via one-way ANOVA test with Tukey's multiple comparisons test. **(C)** Representative images of Masson's trichrome staining of humanized NSG mouse lung at day 63 after IPF cell injection and therapeutic (D35-63) treatment with either KB243 or KB004. Shown are images taken at 50x (top) and 200x (bottom) magnification. **(D)** From left to right, human $CD45^+$, $CD45^+$ $CCR10^+$, $CD45^-$ $EpCAM^+$, $CD45^-$ $EpCAM^+$ $CCR10^+$, and $Lin^-$

272 CCR10$^{+}$ cells in NSG mouse lungs at day 63 after IPF cell injection and treatment with
273 either KB243 (top) or KB004 (bottom); n=4-5/group. **(E-G)** Depicted is the average
274 number of CD45$^{+}$ CCR10$^{+}$ (**E**), EpCAM$^{+}$ CCR10$^{+}$ (**F**), and Lin$^{-}$ CCR10$^{+}$ (**G**) cells and fold
275 change in the levels of mouse *Il6* mRNA (**H**) in NSG lungs at day 63 after IPF cell injection
276 and therapeutic (D35-63) treatment with either KB243 or KB004. Data shown are mean
277 ± s.e.m.; n=4-5/group. *$p \leq 0.05$ via via one-way ANOVA test with Tukey's multiple
278 comparisons test.
279
280
281
282
283
284
285

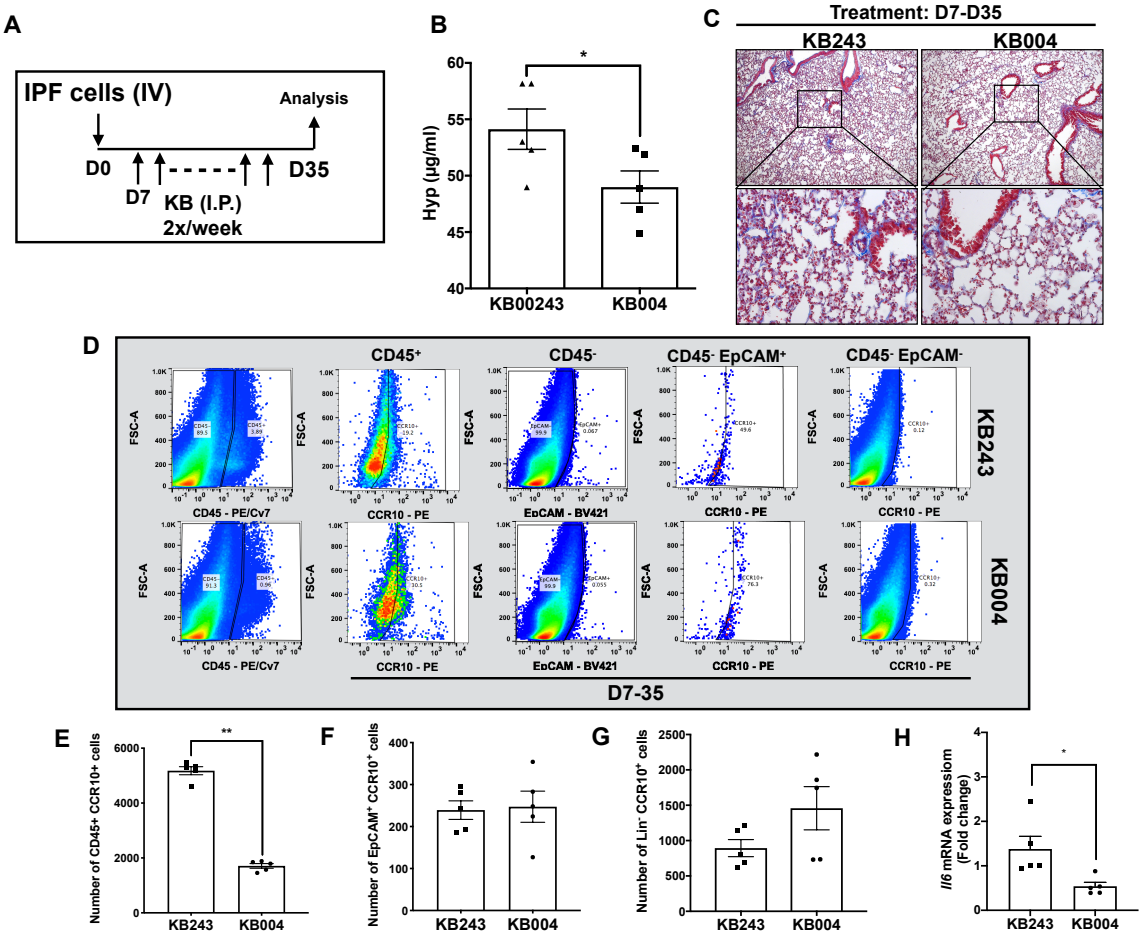


286

287 ***Supplemental Figure 9. Early administration of KB004 significantly ameliorated***

288 ***lung remodeling in humanized NSG mice.***

289 **(A)** Experimental scheme. **(B)** Hydroxyproline in lungs from humanized NSG mice

290 therapeutically (D7-35) treated with either KB243 or KB004 mAbs. Data shown are mean

291 ± s.e.m.; n=5/group *p ≤ 0.05 via one-tailed Mann Whitney non-parametric test. **(C)**

292 Representative images of Masson's trichrome staining of humanized NSG mouse lung at

293 day 35 after IPF cell injection and therapeutic (D7-35) treatment with either KB243 or

294 KB004. Shown are images taken at 50x (top) and 200x (bottom) magnification. **(D)** From

295 left to right, human $CD45^+$, $CD45^+$ $CCR10^+$, $CD45^-$ $EpCAM^+$, $CD45^-$ $EpCAM^+$ $CCR10^+$,

296 and $Lin^-$ $CCR10^+$ cells in NSG mouse lungs at day 35 after IPF cell injection and

297 therapeutic (D7-35) treatment with either KB243 or KB004; n=4-5/group. **(E-G)** Human
298 $CD45^+$ $CCR10^+$ (**E**), $EpCAM^+$ CCR10 (**F**), and $Lin^-$ $CCR10^+$ (**G**) cells and fold change in
299 the levels of mouse *Il6* mRNA (**H**) in NSG mice at day 35 after IPF cell injection and
300 therapeutic (D7-35) treatment with either KB243 or KB004. Data shown are mean ±
301 s.e.m.; n=4-5/group. **$p \leq 0.01$ via two-tailed Mann Whitney non-parametric test.
302
303
304
305
306
307
308

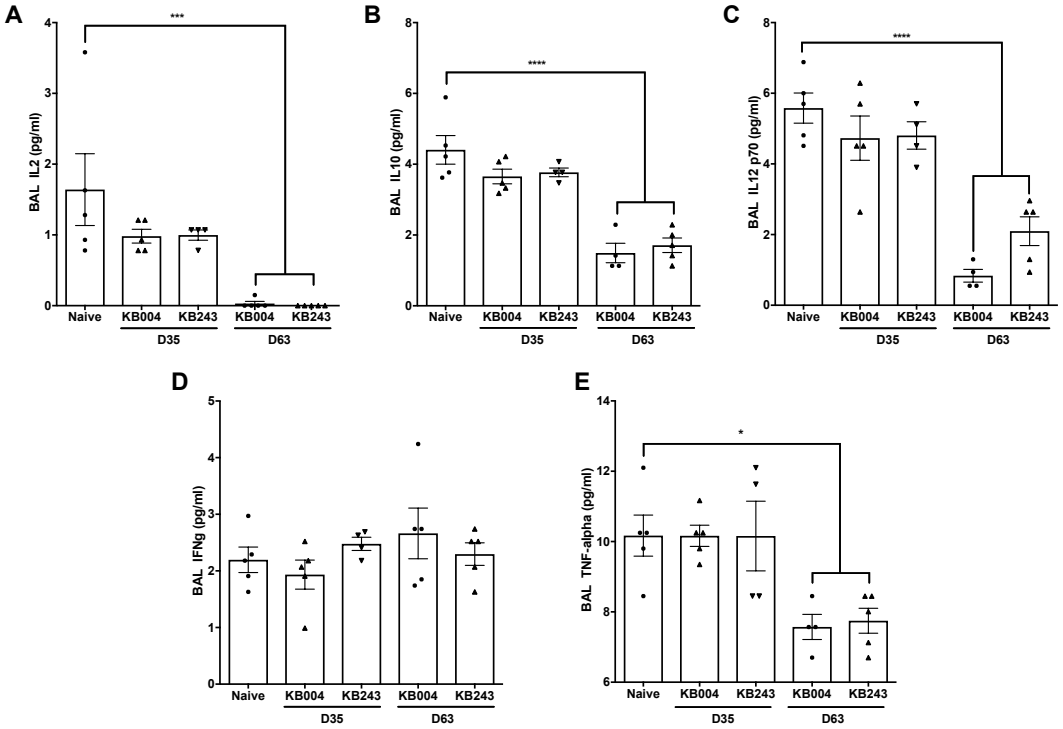


***Supplemental Figure 10. IPF lung cells did not promote inflammation in the NSG mouse.***

**(A-E)** Murine IL-2 (**A**), IL-10 (**B**), IL12-p70 (**C**), IFN$\gamma$, and TNF$\alpha$ in the BAL from non-humanized and humanized NSG mice treated with KB004 or KB243 from days 0 to 35, or from days 35 to 63 after IPF cell injection. Mouse cytokines were measured using Bioplex and data shown are mean $\pm$ s.e.m.; n=5-10/group. *$p \leq 0.05$; ***$p \leq 0.001$ ****$p \leq 0.0001$ via one-way ANOVA with Dunnett correction.

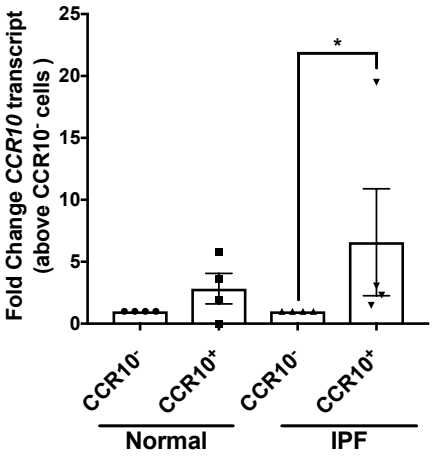


317

318 ***Supplemental Figure 11. Enrichment for CCR10 transcript in magnetically sorted***

319 ***CCR10⁺ cells.***

320 Flow cytometry antibodies for CCR10 were validated by magnetic antibody-mediated

321 purification of CCR10 expressing (i.e. $CCR10^+$) cells from normal and IPF lung explants

322 followed by RNA extraction and qPCR analysis for the chemokine receptor in the sorted

323 cells. Depicted is the average expression of CCR10 transcript in the sorted cells

324 compared with non-sorted cells. Data are mean ± sem; n=4. *$p \leq 0.05$ via two-tailed Mann

325 Whitney non-parametric test.

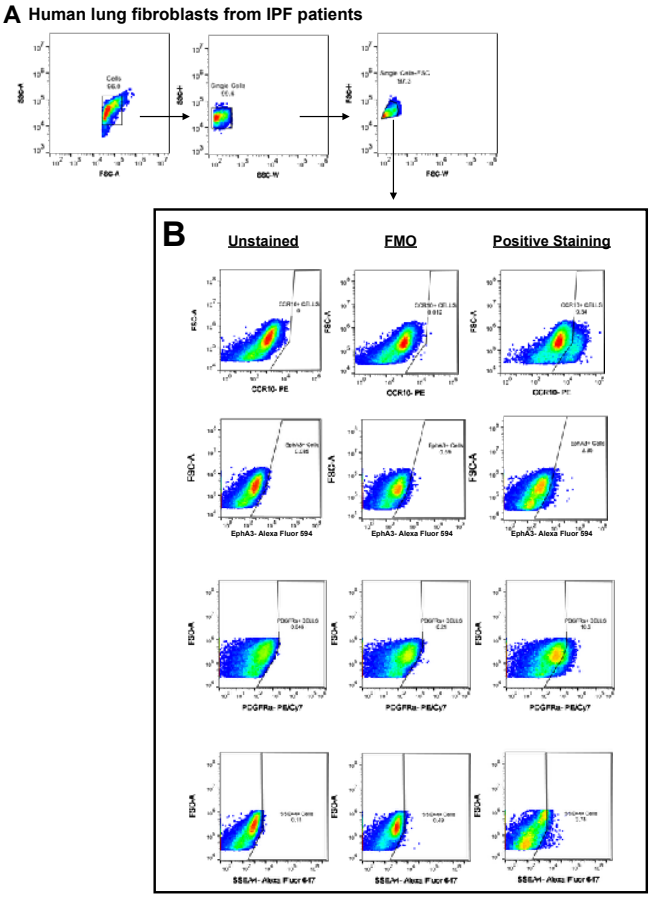


326

327 ***Supplemental Figure 12. Flow cytometric gating strategy of human lung***

328 ***fibroblasts.***

329 **(A)** Gating of human lung fibroblasts from IPF patients shown as a representation of the

330 gating applied for flow cytometric analysis of normal and IPF human lung fibroblast. **(B)**

331 Depicted are representative flow cytometric dot plots for human CCR10, EpHA3, SSEA4,

332 and PDGFRα gates that were determined based upon respective flow cytometric

333 unstained and staining controls (Fluorescence minus one (FMO) and positive staining).

334

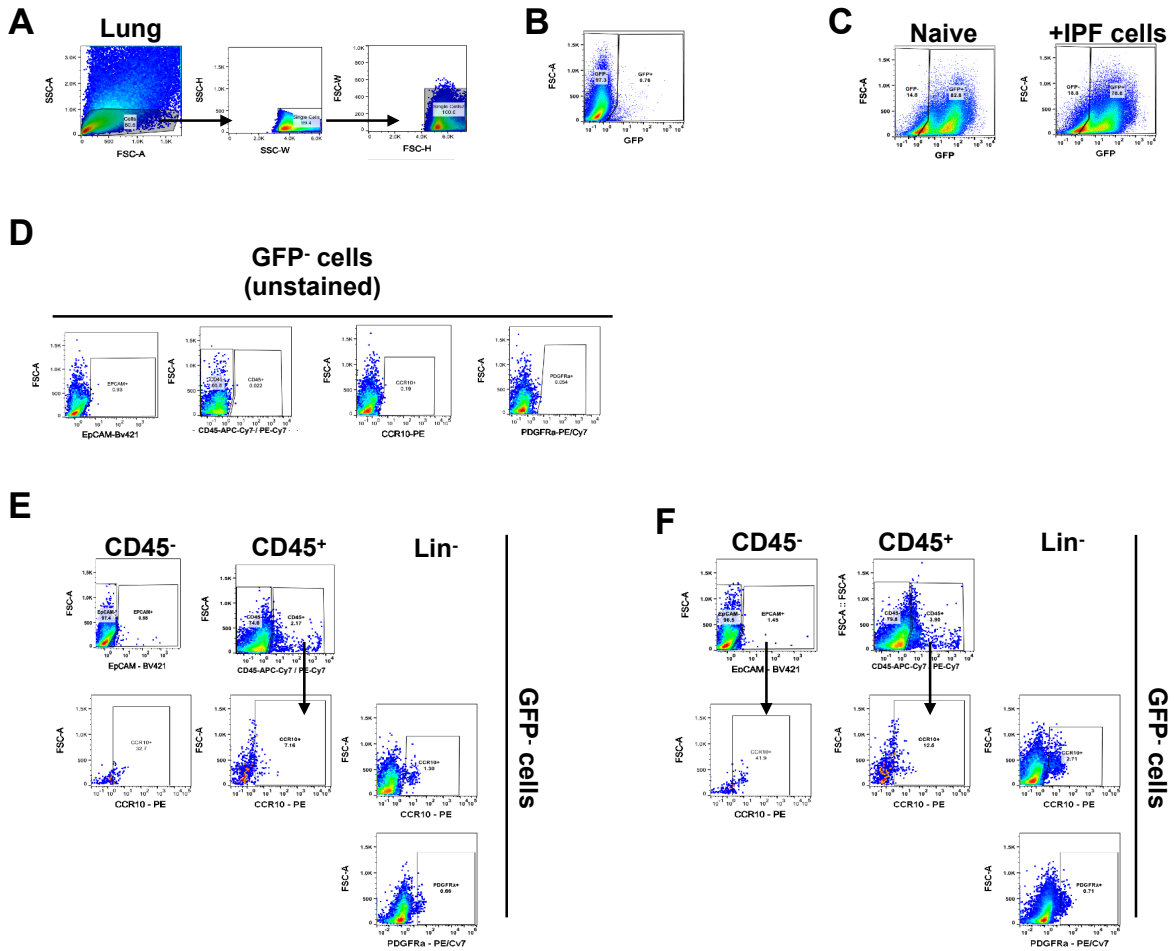


335

336 ***Supplemental Figure 13. Flow cytometric gating strategy of human cells in the***

337 ***lungs of GFP-NSG mice.***

338 Human GFP$^-$ cells were detected in the lungs of GFP-NSG mice at day 35 after IPF cell

339 injection using flow cytometry. **(A)** Gating of cells of interest. **(B)** GFP$^-$ mouse cells from

340 wildtype mice were used to determine both the GFP$^+$ and GFP$^-$ gates. **(C-D)** Human

341 CD45, EpCAM, CCR10, and PDGFRα gates were determined based upon any

342 background staining observed with the anti-human antibodies in non-humanized mice

343 and respective flow cytometry controls. Depicted are representative flow cytometric dot

344 plots for various human cell types present in GFP-NSG the lungs of naïve mice **(E)** or

345 mice that received IPF cells 35 days previously **(F)**.

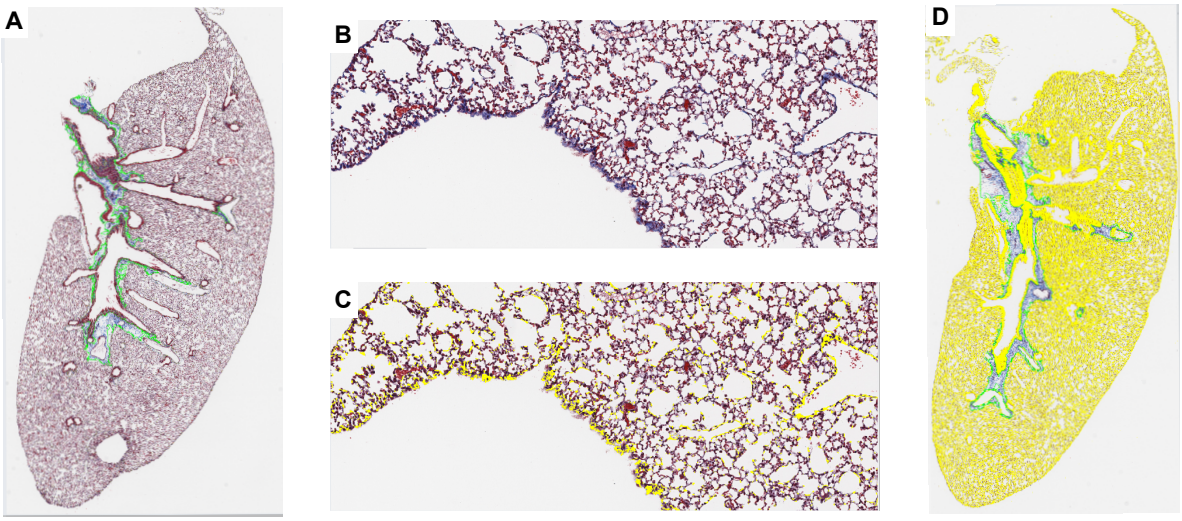


***Supplemental Figure 14. Quantification of interstitial Masson's Trichrome-blue staining.***

Lung tissues were Masson's trichrome stained and tile images of the stained NSG lungs were acquired using a Zeiss AX10 microscope, stitched and exported using Zen 2012 (blue edition) v 1.1.2.0 software. Images were then imported into Image pro premier v9.3.3. (**A-C**) Using image pro, regions of interest (ROI) around large airways and vessels were created (based on the size and blue color of these regions; and the area sum of interstitial trichrome blue staining (**B**) was quantified outside these ROIs (yellow overlay, **C**). This was then normalized to the total area of lung tissue outside the ROIs (yellow overlay, **C**).

358 Supplemental Table 1: IPF patient demographics.

| Patient ID | Age | Sex | Diagnosis | Progression | Therapy at time of explant | Analysis |
|---|---|---|---|---|---|---|
| IPF09-14 | 71 | Male | IPF | Slow | Participated in PRM-151 trial | NSG mice, Flow Cytometry, in vitro analysis |
| IPF10-14 | 70 | Male | IPF | Unknown | Unknown | Flow Cytometry |
| IPF11-14 | 73 | Male | IPF | Unknown | Unknown | Flow Cytometry, in vitro analysis |
| IPF12-14 | 52 | Male | IPF | Unknown | Unknown | Flow Cytometry |
| IPF14-14 | 64 | Male | IPF | Rapid | N-acetylcysteine | NSG mice, Flow Cytometry, in vitro analysis |
| IPF01-15 | 72 | Male | IPF | Unknown | Unknown | Flow Cytometry |
| IPF02-15 | 64 | Male | IPF | Unknown | cefepime, azithromycin, slow steroid taper with Bactrim prophylaxis and Pirfenidone taper | NSG mice, Flow Cytometry, in vitro analysis |
| IPF03-15 | 68 | Female | IPF | Unknown | Unknown | NSG mice, Flow cytometry |
| IPF04-15 | 67 | Male | IPF | Unknown | Pirfenidone | Flow Cytometry, in vitro analysis |
| IPF06-15 | 72 | Female | IPF | Unknown | Unknown | Flow Cytometry |
| IPF01-16 | 58 | Female | IPF | Unknown | Unknown | Flow Cytometry |
| IPF02-16 | 58 | Male | IPF | Unknown | Nintedanib | Flow Cytometry, in vitro analysis |
| ILD03-16 | 58 | Male | IPF | Unknown | Unknown | Flow Cytometry, in vitro analysis |
| IPF04-18 | 65 | Female | IPF | Unknown | Unknown | Flow Cytometry, in vitro analysis |
| IPF05-18 | 65 | Male | IPF | Unknown | Unknown | Flow Cytometry, in vitro analysis |
| IPF08-18 | 49 | Female | IPF | Unknown | Unknown | Flow Cytometry, in vitro analysis |
| IPF09-18 | 64 | Male | IPF | Unknown | Unknown | Flow Cytometry, in vitro analysis |
| IPF10-18 | 66 | Male | IPF | Unknown | Unknown | In vitro analysis |
| IPF11-18 | 61 | Female | IPF | Unknown | Unknown | In vitro analysis |
| IPF15-18 | 65 | Female | IPF | Unknown | Unknown | In vitro analysis |

| | | | | | | |
|---|---|---|---|---|---|---|
| IPF01-19 | 65 | Female | IPF | Unknown | Unknown | Flow Cytometry, in vitro analysis |
| IPF04-19 | 64 | Male | IPF | Unknown | Unknown | In vitro analysis |
| IPF07-19 | 69 | Male | IPF | Unknown | Unknown | In vitro analysis |

362 Supplemental Table 2. Transcript expression of fibrosis-related tyrosine kinases that are

363 not targeted by nintedanib in IPF lung explants

364

365

| Transcript | Fold Change | p value |
|---|---|---|
| *EPHA3* | 10.622 | 0.000019 |
| *DDR1* | 3.312 | 0.00000227 |
| *NTRK2* | 3.242 | 0.0278 |
| *PTK2* | 2.81 | 0.00000954 |
| *ERBB3* | 2.376 | 0.000935 |
| *ERBB2* | 2.252 | 0.0000766 |
| *STYK1* | 2.216 | 0.0133 |
| *EPHB3* | 2.036 | 0.0000573 |
| *TNK2* | 1.965 | 0.00278 |
| *CDK1* | 1.901 | 0.0105 |
| *CSF1R* | 1.876 | 0.0124 |
| *PTK7* | 1.844 | 0.00175 |
| *RET* | 1.79 | 0.000109 |
| *ROR2* | 1.759 | 0.00456 |
| *ZAP70* | 1.652 | 0.0568 |
| *PTK6* | 1.633 | 0.00565 |
| *MST1R* | 1.605 | 0.00379 |
| *EPHB2* | 1.57 | 0.0113 |
| *ERB4* | 1.473 | 0.058 |
| *TYK2* | 1.427 | 0.00752 |

| | | |
|---|---|---|
| *EPHA2* | 1.388 | 0.181 |
| *PTK2B* | 1.376 | 0.119 |
| *DDR2* | 1.354 | 0.31 |
| *TIE1* | 1.343 | 0.297 |
| *LMTK3* | 1.343 | 0.138 |
| *MATK* | 1.337 | 0.0171 |
| *EPHB6* | 1.336 | 0.201 |
| *KIT* | 1.278 | 0.425 |
| *EPHA1* | 1.261 | 0.295 |
| *MET* | 1.241 | 0.49 |
| *ABL1* | 1.221 | 0.295 |
| *AXL* | 1.216 | 0.278 |
| *ITK* | 1.206 | 0.565 |
| *BTK* | 1.204 | 0.436 |
| *EPB1* | 1.182 | 0.174 |
| *RYK* | 1.14 | 0.339 |
| *EPHB4* | 1.137 | 0.238 |
| *CDK4* | 1.137 | 0.327 |
| *TNK1* | 1.105 | 0.469 |
| *TXK* | 1.098 | 0.635 |
| *NTRK1* | 1.061 | 0.669 |
| *INSRR* | 1.048 | 0.62 |
| *CSK* | 1.004 | 0.975 |
| *HCK* | -1.041 | 0.925 |
| *FRK* | -1.05 | 0.878 |

| | | |
|---|---|---|
| *SRMS* | -1.064 | 0.484 |
| *FES* | -1.071 | 0.81 |
| *IGF2R* | -1.106 | 0.72 |
| *TYRO3* | -1.132 | 0.35 |
| *TEC* | -1.133 | 0.327 |
| *FGR* | -1.135 | 0.681 |
| *EPHA8* | -1.144 | 0.315 |
| *ABL2* | -1.201 | 0.447 |
| *EPHA10* | -1.208 | 0.149 |
| *ALK* | -1.258 | 0.191 |
| *EPHA6* | -1.267 | 0.141 |
| *MUSK* | -1.267 | 0.104 |
| *AATK* | -1.292 | 0.0824 |
| *EPHA7* | -1.34 | 0.0603 |
| *LTK* | -1.345 | 0.218 |
| *EPHA4* | -1.396 | 0.171 |
| *EPHA5* | -1.421 | 0.0257 |
| *INSR* | -1.425 | 0.0799 |
| *BLK* | -1.452 | 0.0135 |
| *JAK2* | -1.545 | 0.0329 |
| *ROS1* | -1.548 | 0.171 |
| *FER* | -1.549 | 0.0159 |
| *SYK* | -1.559 | 0.0333 |
| *JAK3* | -1.584 | 0.148 |
| *MERTK* | -1.618 | 0.0908 |

| | | |
|---|---|---|
| *YES1* | -1.733 | 0.00758 |
| *IGF1R* | -1.747 | 0.0371 |
| *CDK2* | -1.954 | 0.00915 |
| *LMTK2* | -2.04 | 0.0006 |
| *EGFR* | -2.041 | 0.00611 |
| *NTRK3* | -2.056 | 0.0197 |
| *FLT3* | -2.146 | 0.000138 |
| *FYN* | -2.25 | 0.000848 |
| *ROR1* | -2.44 | 0.00638 |
| *TEK* | -2.803 | 0.0041 |
| *JAK1* | -2.958 | 0.000982 |

366
367

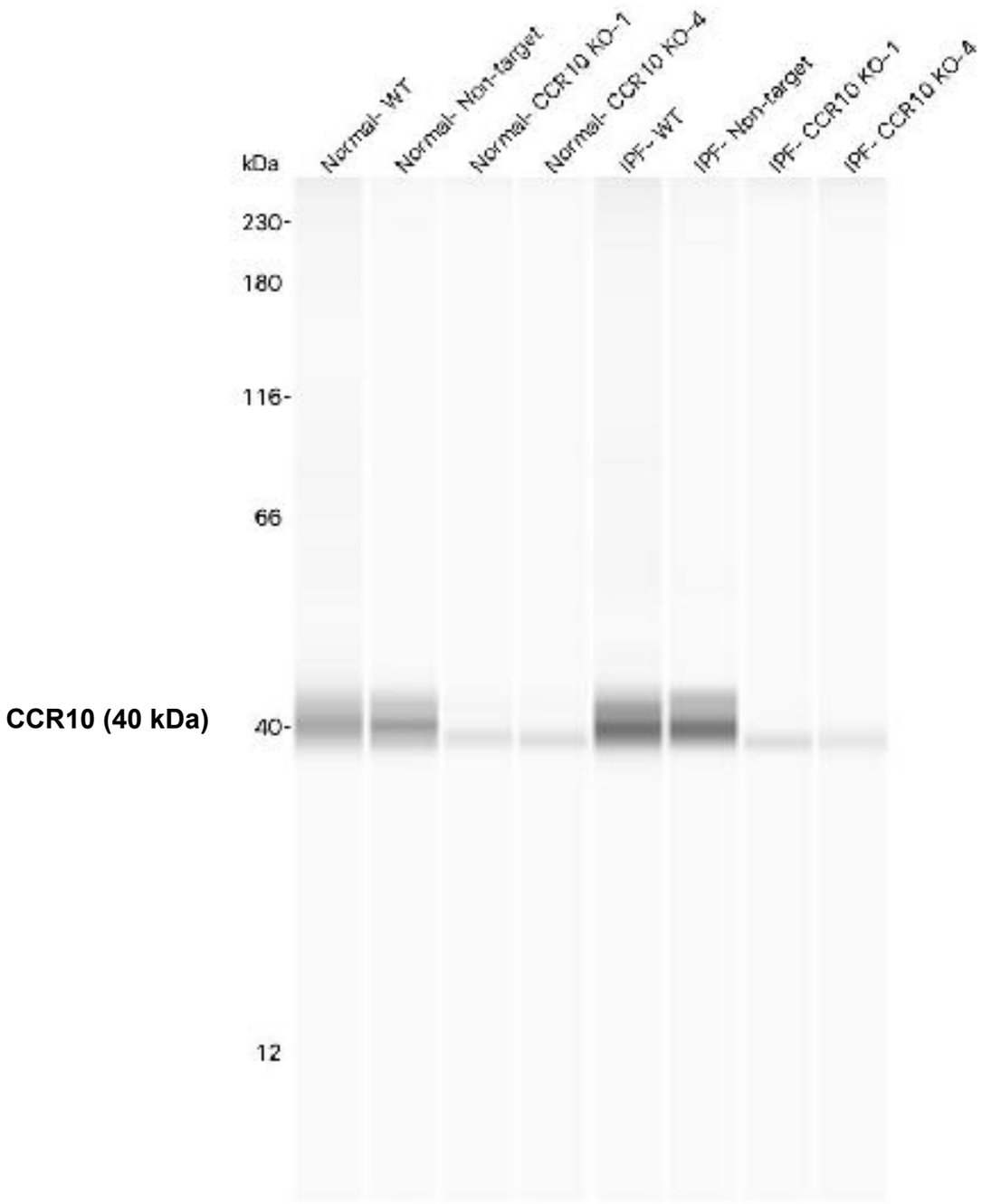
kDa
Normal- WT
Normal- Non-target
Normal- CCR10 KO-1
Normal- CCR10 KO-4
IPF- WT
IPF- Non-target
IPF- CCR10 KO-1
IPF- CCR10 KO-4
230-
180
116-
66
CCR10 (40 kDa)
40-
12

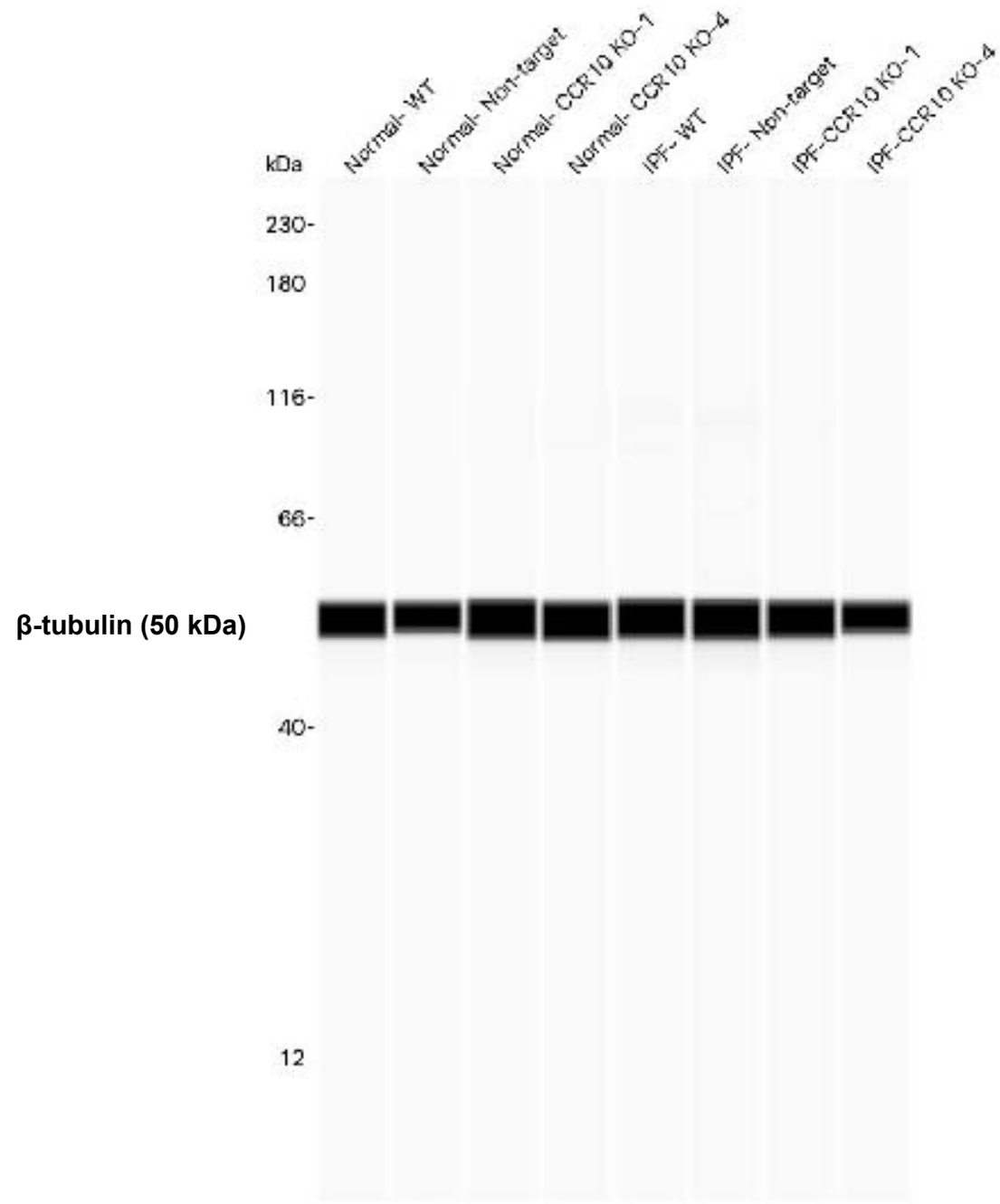
kDa
Normal- WT
Normal- Non-target
Normal- CCR10 KO-1
Normal- CCR10 KO-4
IPF- WT
IPF- Non-target
IPF-CCR10 KO-1
IPF-CCR10 KO-4
230-
180
116-
66-
β-tubulin (50 kDa)
40-
12